High pressure effects on U L_3 x-ray absorption in partial fluorescence yield mode and single crystal x-ray diffraction in the heavy fermion compound UCd_{11}

Farzana Nasreen[1*], Daniel Antonio[1], Derrick VanGennep[2], Corwin H. Booth[3], Karunakar Kothapalli[4], Eric D. Bauer[5], John L. Sarrao[5], Barbara Lavina[1], Valentin Iota-Herbei[1], Stanislav Sinogeikin[6], Paul Chow[6], Yuming Xiao[6], Yusheng Zhao[1], Andrew L. Cornelius[1]

[1] *High Pressure Science and Engineering Center (HiPSEC) and Department of Physics and Astronomy, University of Nevada, Las Vegas, NV 89154, USA*

[2]*Department of Physics, University of Florida, Gainesville, FL 32611, USA*

[3]*Chemical Sciences Division, Lawrence Berkeley National Laboratory, Berkeley, California, 94720, USA*

[4]*Ames Laboratory, U.S. DOE and Department of Physics and Astronomy, Iowa State University, Ames, Iowa 50011, USA*

[5]*Los Alamos National Laboratory, P. O. Box 1663, MS K764, Los Alamos, NM, 87545, USA*

[6]*High Pressure Collaborative Access Team, Carnegie Institution of Washington, Argonne National Laboratory, Argonne, Illinois 60439, USA*

Abstract

We report a study of high pressure x-ray absorption (XAS) performed in the partial fluorescence yield mode (PFY) at the U L_3 edge (0-28.2 GPa) and single crystal x-ray diffraction (SXD) (0-20 GPa) on the UCd_{11} heavy fermion compound at room temperature. Under compression, the PFY-XAS results show that the white line is shifted by +4.1(3) eV at the highest applied pressure of 28.2 GPa indicating delocalization of the 5*f* electrons. The increase in full width at half maxima (FWHM) and decrease in relative amplitude of the white line with respect to the edge jump point towards 6*d* band broadening under high pressure. A bulk modulus of K_0 = 62(1) GPa and its pressure derivative, K_0' = 4.9(2) was determined from high pressure SXD results. Both the PFY-XAS and diffraction results do not show any sign of a structural phase transition in the applied pressure range.

PACS number: 78.70.Dm, 71.27.+a, 62.50.-p, 62.20.de

Keywords: High pressure, x-ray absorption, single crystal x-ray diffraction, uranium intermetallic, heavy-fermion, UCd_{11}.

*Corresponding Author:

Farzana Nasreen
University of Nevada, Las Vegas
HiPSEC and Department of Physics & Astronomy
Box 454002
4505 Maryland Parkway
Las Vegas, NV 89154-4002, USA
Phone no: +1-575-202-9344
Fax:+1+702- 895-0804
Email: farzana6109@gmail.com

1. Introduction

The wide range of ground state properties exhibited by uranium intermetallics - including heavy fermion behavior, complex magnetic structures, unconventional superconductivity and non-Fermi liquid behavior – are related to the degree of localization of the 5*f* electronic states that vary from strongly localized, as seen in lanthanides, to itinerant, as seen in transition metals. Unlike 4*f* electrons, which remain close to the atomic core, the 5*f* electrons have a large spatial extent, and as a result they interact strongly with the neighboring ligand orbitals and conduction band. The variable degree of localization determined by the local environment leads to competing interactions [1, 2]. In fact, uranium compounds generally follow an empirical critical limit called *Hill* limit (3.4-3.6 Å), where the compounds with uranium interatomic distances (d_{U-U}) larger than this limit show magnetic behaviour similar to those of rare earth elements, while compounds where d_{U-U} is within the *Hill* limit show itinerant behavior, such as Pauli paramagnetism where 5*f* electrons are significantly delocalized [3]. A delicate balance between these different interactions leads to diverse structural, magnetic, and electronic properties. This balance can be altered by changing chemical composition or applying pressure and/or a magnetic field. Hydrostatic pressure is an important "clean" non-thermal parameter (i.e., not expected to introduce chemical disorder) to systematically study uranium intermetallic systems as pressure causes a reduction in interatomic distance and hence increases the electron density in the compressed lattice. As a result pressure can cause an increase of the 5*f*-5*f* hybridization as well as the 5*f*-ligand hybridization, thus moving the 5*f*-states towards delocalization. Such a change in the nature of the 5*f* state can drastically alter the electronic, structural and magnetic properties and can lead to exotic behaviour such as volume collapse transitions, mixed valency and superconductivity [4-6].

UCd_{11} is an excellent candidate for studying the effect of pressure on a strongly localized heavy-fermion uranium intermetallic, as it is one of the most intriguing of all the binary uranium compounds that have been discovered so far. It crystallizes in the cubic $BaHg_{11}$-type structure with a lattice constant of 9.29 Å [7]. The nearest U-U neighbor distance of 6.56 Å is very large compared to the *Hill limit* [3] and overlapping of neighboring 5*f* wavefunctions is expected to be minimal. UCd_{11} follows the *Hill* criterion for the formation of magnetic ground state and orders antiferromagnetically at $T_N \approx 5$ K [7] with a complex magnetic state [8]. Ambient pressure magnetic susceptibility above 80 K follows a Curie-Weiss law with an effective magnetic moment of $\mu_{eff} = 3.45\ \mu_B$/U, whereas below 80 K it deviates from the Curie-Weiss law and finally attains a constant value below 5 K [7]. Low-temperature resistivity, specific heat and magnetization in an applied magnetic field and/or under hydrostatic

pressure revealed additional transitions below 5 K to a complex magnetic ground state [9-12]. Its electronic specific heat coefficient known as Sommerfeld coefficient, γ = 803 mJ/mol-K^2, in the paramagnetic region, is the highest for any ordered uranium heavy fermion system [13]. The extrapolated zero temperature Sommerfeld coefficient, γ_0, is one-third of the γ in the paramagnetic region, indicating a partial removal of a heavy quasiparticle from the Fermi surface, consistent with de Has-van Alphen (dHvA) measurement [14]. A similar reduction in γ_0 in the ordered state is found in many other U-based heavy fermion magnetic compounds with different antiferromagnetic structure [15]. Recent reports of specific heat measurements on UCd_{11} show a transfer of magnetic specific heat to electronic specific heat consistent with a many-body Kondo effect [16].

Although lanthanide (Ln) L_3 edge high resolution PFY-XAS measurements under applied pressure are routinely utilized as a bulk probe to determine the Ln valence under pressure [17], the use of this technique on actinide (An) materials has been limited. The limitation is partly because of large $3d_{5/2}$ core-hole lifetime broadening (about ~ 3.9 eV for uranium compared to that of 0.8 – 1.5 eV in lanthanides [18-20]) and the decrease in the energy separation of different 5*f* configurations features in An L_3 edge spectra ($\leq$ 5eV in light actinides compared to 8-10 eV in lanthanides [17, 21, 22]). Furthermore, interpretation of U L_3 PFY-XAS is more complicated because the ability of 5*f* orbitals to screen the core-hole can vary from compound to compound due to its varying degrees of delocalization, in contrast to the effective screening by the more reliably localized 4*f* orbitals in different Ln compounds [21, 22]. Nevertheless, a shift in the so-called "white line" (the intense peak immediately following the absorption edge) in the L_3 edge PFY-XAS technique under high pressure in actinides may still provide valuable information related to the degree of delocalization of 5*f* electrons and can be combined with high pressure diffraction measurements to extract complementary compressibility data to relate 5*f* delocalization to the relative change in lattice volume. Therefore, employing high resolution PFY-XAS under high pressure can be useful for studying *f*-orbital behavior in actinides, as well as lanthanides. With this goal in mind, we selected the heavy fermion compound UCd_{11}, which stands out in the uranium intermetallic series with magnetic order for its very high value of electronic specific heat, indicative of a strongly localized *f* orbital, as discussed below.

A clear correlation has been found in uranium and plutonium intermetallic systems between γ and ΔE_α, where ΔE_α is the shift in the white line position of uranium and plutonium compounds with respect to the position of elemental α-U and α-Pu respectively [21]. Based on this correlation, UCd_{11} has both the highest γ and the largest shift ΔE_α ~ -6.5 eV among the studied group of uranium compounds in Ref. 22. A high Sommerfeld coefficient is a

hallmark of heavy fermion behavior as it is proportional to effective carrier mass, which in turn is proportional to the density of states at the Fermi level [23]. Since a flat, atomic-like band corresponds to a high γ, the specific heat is commonly used as a rough measure of delocalization. White line energy shifts are perhaps a more direct measure of delocalization, as a localized orbital will screen the $2p_{3/2}$ core hole from the outgoing photoelectron in an L_3 edge experiment, reducing the Coulomb interaction between the photoelectron and the core hole, thus lowering the threshold energy for excitation and increasing ΔE_α. More detailed results can be obtained from the related resonant x-ray emission spectroscopy (RXES) technique, and recent measurements on UCd_{11} were interpreted in terms of the multiconfigurational nature of 5*f* state orbitals [21]. It is reported that the 5*f* orbital has a total occupancy of 2.7 ± 0.2 ($5f^1$ = 0.07 ± 0.007, $5f^2$ = 0.15 ± 0.015, $5f^3$ = 0.78 ± 0.078) and therefore may not be in a purely $5f^3$ (U^{3+}) configuration. Such a multiconfigurational state has also been reported in $UCoGa_5$, α-Pu, δ-Pu, $PuCoIn_5$, $PuCoGa_5$ and $PuSb_2$ through RXES measurements [21, 22]. PFY-XAS measurement at U L_3 edge not only provides bulk sensitivity, element and orbital selectivity but it can also provide sharp spectral features by overcoming core-hole life time broadening. In traditional U L_3 edge x-ray absorption near edge spectroscopy (XANES) the incident photon is absorbed by a $2p_{3/2}$ core electron and is promoted to an unoccupied uranium 6*d* state above the Fermi level (E_F). Therefore the resolution is dominated by $2p_{3/2}$ core-hole lifetime broadening (about ~ 7.4 eV for uranium) [19, 20]. Unlike traditional XANES, PFY-XAS utilizes a high-resolution x-ray emission spectrometer to record the intensity of the $L_{\alpha 1}$ fluorescence line ($3d_{5/2} \rightarrow 2p_{3/2}$) as function of incident energy varied around U L_3 edge (17.166 keV), resulting in a spectrum with higher resolution limited by $3d_{5/2}$ core hole life time broadening (~ 3.9 eV) [20]. Here, we report on the effect of high pressure on the uranium L_3 x-ray absorption in partial fluorescence yield mode (PFY-XAS) and single crystal x-ray diffraction (SXD) measurements in the UCd_{11} heavy fermion compound.

2. Experiment

Single crystals of UCd_{11} were grown by the molten metal flux growth technique [24]. X-ray diffraction confirmed single-phase material crystallizing in the cubic $BaHg_{11}$ structure (space group: *Pm-3m*). UCd_{11} has a caged structure with the uranium atom surrounded by 16 cadmium atoms. The uranium occupies the 3*c* position having tetragonal symmetry and has 12 nearest-neighbors and 8 next-nearest neighbor Cd atoms. The nearest U-U neighbor distance is 6.56 Å and nearest U-Cd distance is 3.45 Å at ambient conditions. The crystal structure and the nearest-neighbor and the next-nearest-neighbor environments of uranium atoms are shown in Figure 1.

2.1. X-ray absorption in partial fluorescence yield mode (PFY-XAS)

High pressure uranium L_3 edge x-ray absorption spectra in partial fluorescence yield mode (PFY-XAS) were taken on HPCAT 16-ID-D undulator beamline at the Advance Photon Source (APS). A monochromatic x-ray beam was obtained using a Si (111) double crystal monochromator, focused to a beam size of 25×55 μm^2 with meter-long horizontal and vertical Kirkpatrick-Baez mirrors. A Paderborn-panoramic style diamond anvil cell (DAC), equipped with Boehler-Almax anvils of 300 µm culet diameter and a beryllium gasket, was used to apply high pressure. The beryllium gasket was pre-indented to 50 µm thickness and a 100 µm diameter hole was drilled to serve as a sample chamber. Two annealed ruby spheres of ~ 5 µm diameter were placed in the gasket hole along with the sample as a pressure calibrant. A ~ 30 µm thick sample was used. A 4:1 methanol-ethanol mixture was loaded as a pressure transmitting medium. Radial scattering geometry was employed, where the incoming x-ray beam entered through the Be gasket in the radial direction and the secondary emission from the sample passed through the Be gasket to the spectrometer analyzer. Due to safety regulations ambient data was not taken on the same sample inside the pressure cell. Therefore a separate sample of 15 µm thickness was used to take ambient PFY-XAS data. A Rowland circle spectrometer was used to analyze the secondary emitted fluorescence beam from the sample. The spectrometer was comprised of a spherically bent Si (844) single crystal analyzer and Peltier-cooled silicon detector (AMPTEK XR_100CR). The spectrometer utilized the Rowland circle geometry where the sample, the single crystal analyzer (1 meter bend radius) and the detector all lie on the perimeter of the Rowland circle with a diameter of 1 meter. For PFY-XAS measurements, the intensity of the U $L_{\alpha 1}$, ($3d_{5/2} \rightarrow 2p_{3/2}$) (13.614 keV) fluorescence line is measured as a function of the incident photon energy varied around the U L_3 absorption edge (17.166 keV). The acquisition time for each PFY-XAS spectrum at a given pressure was 20 minutes. The energy resolution of the incoming beam was about 2.2 eV and the spectrometer energy resolution was about ~ 0.7 eV, giving a total estimated energy resolution of 2.3 eV. More detailed explanation on the experimental setup can be found in Ref. 25. The sample was aligned to minimize self-absorption. Ideal sample size for XAS measurements in fluorescence mode should be either sufficiently thin or dilute to avoid self-absorption from the outgoing emitted beam [26]. The sample inside the pressure cell was 30 µm thick whereas the sample used for ambient data was 15 µm thick. Although corrections for self-absorption effects exist in the thick limit, our samples were too thin to be considered in the thick limit; that is, they are in the intermediate thickness limit where correction factors do not currently exist. Consequently, there is no way to correct the in-cell data and the out-cell data. However, although the two samples differ in thickness by 15 µm, a comparison between our data from the two samples and with the data in

Ref. 21. is reasonably good. Note that this correction is important primarily for comparing the ambient pressure data to the applied-pressure data sets.

2.2 Single crystal x-ray diffraction

For high pressure single crystal x-ray diffraction measurements at room temperature, a four-post wide-opening DAC equipped with Boehler-Almax diamond anvils of 600 µm culet diameter and a 70° aperture was used. A single crystal of UCd_{11} (100 x 120 µm ^{2}) was loaded into a rhenium (Re) gasket with preindented thickness of 70 µm and a 200 µm diameter drilled hole. Two annealed ruby spheres of ~ 5 µm diameter were placed in the gasket hole along with the sample as pressure calibrant. A 4:1 methanol-ethanol mixture was loaded as a pressure transmitting medium in the DAC just as in the PFY-XAS measurements. This pressure transmitting medium is hydrostatic up to the freezing pressure of 10.4 GPa and it shows nearly hydrostatic behaviour up to a pressure of 20 GPa [27].

High-pressure single crystal x-ray diffraction data were collected at the HPCAT 16-ID-B undulator beamline at APS. The data were collected in the range 0-20 GPa with the rotation method with a monochromatic x-ray beam of λ = 0.4066 Å from a Si (111) double crystal monochromator. The diffraction patterns were collected using a 165 MAR CCD area detector, which was calibrated using a CeO_2 standard through Fit2D software [28]. At each pressure a wide scan in ω in the range ± 38° as well as a step scan of 1° interval in the same angular range was taken. Each wide scan was also split into 4 intervals of 19° to avoid peaks overlapping. GSE_ADA software [29] was utilized to extract the peak coordinates 2θ, χ and ω. ± 38° wide scan is used to extract the 2θ and χ coordinates whereas the stepped scans of 1° interval were used to extract the maximum intensity at each angle and the third spatial coordinate 'ω' which contains information needed to reconstruct the reciprocal space and index the diffraction pattern. Lattice parameters were determined through least-squares minimization of the d-spacing of all observed peaks using the RSV software [30]. Saturated, overlapping and partial peaks were omitted as well as diamond peaks. More detailed explanation on the experimental station setup can be found in Ref. 31.

3. Results and Discussion

3.1. High Pressure uranium L_3 x-ray absorption in partial fluorescence yield mode (PFY-XAS)

Figure 2 shows the U L_3 PFY-XAS spectra of UCd_{11} collected at pressures ranging from 0 to 28.2 GPa. The oversampled PFY-XAS spectra were smoothed using the Savitzky-Golay filter method choosing a window size of five points and a second order polynomial. The PFY-XAS spectra consist of a white line with an underlying edge

discontinuity. Figure 2 shows the clear shift in the white line towards the high energy side and a decrease in the relative amplitude of the white line with respect to the edge jump as the pressure is increased.

Each spectrum is analyzed by a least-squares fit of a summation of a Gaussian (for the white line with experimental broadening) with an arctan-like step function (integrated pseudo-Voigt) for the edge structure. The white line positon of ambient pressure data is used as a reference to measure the shift (E_{LIII}) in the white line as the pressure is increased. Figure 3 shows a linear increase in the shift (E_{LIII}) with respect to applied pressure with a slope of $dE_{LIII}/dP = 0.15 \pm 0.01$ eV/GPa. At the highest applied pressure of 28.2 GPa, $E_{LIII} = +4.1 \pm 0.3$ eV. The linear increase of E_{LIII} with pressure is consistent with a similar linear increase of the full width at half maxima (FWHM) of the white line resonance under pressure, as shown in Figure 4. FWHM increases by 3.8 eV between 0 and 28.2 GPa. The white line energy position is mainly dominated by the strong Coulomb interaction energy between the 2*p* core-hole and outgoing photoelectron. Pressure can induce delocalization of the 5*f* electrons, effectively reducing the ability of these electrons to screen the core hole, increasing the Coulomb interaction energy and causing the energy for the photoelectron to escape (the white line position) to increase. High pressure x-ray absorption in many uranium compounds such as UTe, UC, UN and UPd_2Al_3 have shown change in slope dE_{LIII}/dP and slope of FWHM around pressure where these compounds are known to undergo structural phase transitions confirmed by x-ray diffraction measurement under high pressure [32-34]. No change in the slope dE_{LIII}/dP and slope of FWHM in UCd_{11} is seen which indicates that UCd_{11} does not go through a phase transition in the measured range of applied pressure and is consistent with SXD data under pressure discussed below in section 3.2. Although finding the 5*f* configuration from the white line shift in PFY-XAS data under pressure is difficult, nevertheless it is interesting to note that the observed shift of +4.1 eV in the white line is equivalent to the edge shift between the known oxidation state U^{4+} ($5f^2$) and U^{3+} ($5f^3$) seen in UF_4 and UCl_3 respectively [35]. Theoretical value of shift (E_{LIII}) for two different 5*f* configurations, U^{4+} ($5f^2$) and U^{3+} ($5f^3$), in uranium metal is reported to be 4.6 eV [36] and is very close to shift seen in UCd_{11}.

Even though the resolution of PFY-XAS spectra is better than conventional XANES, the multiconfigurational nature is not resolved, possibly due to $3d_{5/2}$ core-hole lifetime broadening combined with internal instrument broadening; however, delocalization effects should play an important role in uranium compounds [37]. In addition, recent PFY-XAS and RXES measurements and FEFF simulations on plutonium compounds [22] suggest that the observed shift of +4.1 eV in the white line under pressure in UCd_{11} may also be due

to a shift in 5*f* configurations weight or combination of this effect and delocalization. An interpretation of the shift in the white line under pressure in terms of multiconfigurational nature or 5*f*-6*d* mixing is beyond the scope of this work as RXES data on UCd_{11} under pressure is not currently available. In any case, changes in the features of uranium L_3 white line ultimately reflect on the variation in the unoccupied 6*d* density of states in the final state. Therefore, without ascribing the changes in the absorption characteristics to the exact nature of the electronic structure in UCd_{11}, the increase in FWHM and decrease in relative amplitude of the white line with respect to the edge jump under pressure is related to 6*d* band broadening in the final state. In a given pressure range of 0-28.2 GPa, the white line shift in UPd_2Al_3, UPd_3, UN, UC and UCd_{11} is ≈ 1.8 eV, 0 eV, 0.8eV, 1.2 eV and 4.1 eV respectively [32, 34]. Compared to other uranium intermetallic compound such as UPd_2Al_3, UPd_3, UN and UC shift of the white line in UCd_{11} is very large. Such a large shift under pressure demonstrates that UCd_{11} is a localized 5*f*-system at ambient pressure, becoming significantly more delocalized with increasing pressure.

3.2 High Pressure single crystal x-ray diffraction

Figure 5 shows the variation in the normalized unit cell volume as a function of pressure (P) in the range 0-20 GPa. The ambient pressure volume (V_0) is 801.4 $Å^3$. At highest applied pressure of 20 GPa the volume is reduced by ~ 18% without any sign of a discontinuity, consistent with the PFY-XAS data which also show no evidence of structural phase transitions in this pressure range. A subtle discontinuity at 10.4 GPa, which corresponds to the freezing pressure of 4:1 methanol:ethanol pressure transmitting medium, is seen and is most likely due to the onset of non-hydrostaticity. The volume versus pressure (V-P) data were fitted using 3rd order Birch-Murnaghan (BM) [35] and Vinet [36, 37] equations of state (EOS) shown below in equation (1) and equation (2) respectively.

$$P = \frac{3K_0}{2}\left[\left(\frac{V_0}{V}\right)^{\frac{7}{3}} - \left(\frac{V_0}{V}\right)^{\frac{5}{3}}\right]\left\{1 + \frac{3}{4}(K_0' - 4)\left[\left(\frac{V_0}{V}\right)^{\frac{2}{3}} - 1\right]\right\} \quad (1)$$

$$P = 3K_0\left(\frac{1 - \left(\frac{V}{V_0}\right)^{1/3}}{\left(\frac{V}{V_0}\right)^{2/3}}\right) exp\left\{\frac{3}{2}(K_0' - 1)\left(1 - \left(\frac{V}{V_0}\right)^{1/3}\right)\right\} \quad (2)$$

K_0 denotes the isothermal bulk modulus and K_0' its first pressure derivative. Both equations of state fit the data satisfactorily. Fitting parameters with both equations of state yield similar values of bulk modulus (K_0) and its pressure derivative (K_0'). The value of K_0 = 62(1) GPa is same for both fits and K_0' is 4.9(2) and 5.2(2) for 3rd order

BM EOS and Vinet EOS respectively. The ambient U-U spacing of 6.56 Å is reduced by ~ 6.3% at the highest applied pressure of 20 GPa. Figure 6 shows the single crystal diffraction pattern of UCd_{11} at two different pressures 1.5 GPa and 12.7 GPa. No phase transition can be seen as there is no change in the pattern of reflections at low and high pressure. Figure 7 shows comparison of a peak profile for hkl(??) reflection at the same two pressures points 1.5 GPa and 12.7 GPa.

In a given pressure range from 0 to 20 GPa, the unit cell volume of UBe_{13}, UCd_{11}, UPd_2Al_3, UPd_3 and UTe is compressed by 12 %, 18 %, 9 %, 9 % and 24 % respectively [33, 38, 39, 4]. UTe has highest volume compression as it goes through a phase transition through volume collapse of 10 % at 10 GPa. Compared to other mentioned compounds UCd_{11} shows large compression of volume in 0 to 20 GPa range and would be interesting to investigate at further high pressure to see if it goes through any volume collapse transition. The large decrease in volume is consistent with large shift in white line under pressure. The U-U spacing at the highest pressure is still much higher than the *Hill limit* (3.4-3.6 Å) [3] and therefore the 5*f*-5*f* wavefunction overlap is minimal. Hence 5*f*-4*d* hybridization is still the dominant control parameter for the formation of the ground state. Under compression, the decrease in the U-Cd distance can potentially increase the 5*f*-4*d* hybridization and lead to the delocalization of 5*f* electrons as indicated by the PFY-XAS data under pressure. The parameter $dE_{LIII}/d(lnV)$ indicates the correlation of the shift in the white line to the change in lattice volume and therefore gives a measure of the degree of delocalization of 5*f* electrons with respect to decreasing unit cell volume. A study by Bertram et al. [32] on the U L_{III} edge under pressure of various uranium monochalcogenides is useful for comparisons. For instance, the value of $dE_{LIII}/d(lnV) = 9.3$ for UCd_{11} is comparable that of UTe, which has $(dE(L_3)/d(lnV) = 9.6$ and is a quasi-localized compound with bulk modulus (K_0) = 48.6 GPa and U-U spacing ≈ 4.35 Å [32]. The value of $dE_{LIII}/d(lnV)$ for uranium-pnictides UC and UN with 5*f* itinerant state are 4.7 and 5.7 respectively [32]. The bulk modulus and U-U spacing of UN and UC are 203 GPa and 160 GPa and 3.35 Å and 3.51 Å respectively [32]. It is interesting to note that the shift in the white line energy with decreasing unit cell volume is pronounce more in quasi-localized compound UTe compared to itinerant compound UN and UC. The parameter $dE_{LIII}/d(lnV)$ in UCd_{11} follows this trend and shows that it is a localized compound at ambient pressure and gets significantly delocalized under pressure.

Along with UCd_{11}, other binary heavy fermion uranium intermetallic compounds that have large U-U spacing and low U content are UBe_{13} (d_{U-U} = 5.13 Å) and U_2Zn_{17} (d_{U-U} = 4.39 Å) [7]. Among these, UCd_{11} has the

lowest value of bulk modulus ~ 62 GPa (UBe_{13} = 108 GPa [38], U_2Zn_{17} = 87 GPa [40]. In such compounds the bulk modulus is mostly determined by the large number of transition metal atoms surrounding the uranium atom [38]. Even though the bulk moduli of uranium (114.5 GPa) [41] and thorium (58 GPa) [42] are very different, the bulk moduli of UBe_{13} (108 GPa) [38], $ThBe_{13}$ (107 GPa) [38], and beryllium (109.88 GPa) [43] are very similar and indicate that the bulk modulus of the An-Be_{13}(An=U/Th) compounds is mostly due to the cage-like structure of surrounding beryllium atoms. Similarly, the bulk modulus of U_2Zn_{17} (87 GPa) [40] is comparable to that of zinc (72 GPa) [44]. The bulk modulus of UCd_{11} (62 GPa) follows this trend and is comparable to the bulk modulus of cadmium (41.6 GPa) [44].

4. Conclusions

We have investigated the high pressure behavior of UCd_{11} compound through x-ray absorption in partial fluorescence yield mode (0-28.2 GPa) and single crystal x-ray diffraction (0-20 GPa). The PFY-XAS results show a large shift of +4.1 eV in the white line under pressure due to the delocalization of 5*f* electrons. Likewise, an increase in the white line resonance FWHM and a decrease in relative amplitude with respect to edge jump point towards 6*d* band broadening in the final state. The SXD data under pressure reveals an 18% volume reduction, a bulk modulus 62 GPa, and a U-U distance that remains well above the *Hill limit*. Both the PFY-XAS and diffraction results do not show any sign of a structural phase transition in the applied pressure range. Large changes in PFY-XAS spectral features under high pressure point towards delocalization of the 5*f* orbital, indicating that the *f* electrons are strongly localized at ambient pressure, UCd_{11} is therefore a good system to investigate the local moment behavior of *5f* state through photoemission spectroscopy.

Acknowledgement

We acknowledge fruitful discussion with Ladislav Havela and Jon Lawrence. We thank Curtis Kenney-Benson for his assistance at HPCAT (Sector 16), APS, Argonne National Laboratory (ANL). This work was supported by DOE/EPSCoR (Experimental Program to Stimulate Competitive Research) University/National Laboratory Partnership (DE-SC0005278). The research work at High Pressure Science and Engineering Center (HiPSEC) at University of Nevada at Las Vegas (UNLV) was sponsored by the National Nuclear Security Administration (NNSA) under the Stewardship Science Academic Alliances program through DOE Cooperative Agreement #DE-NA0001982. Work at Lawrence Berkeley National Laboratory supported by the Director, Office of Science, Office of Basic Energy Sciences (OBES), of the U.S. DOE under Contract No. DE-AC02-05CH11231. Portions of this

work were performed at HPCAT (Sector 16), APS, ANL. HPCAT operations are supported by DOE-NNSA under Award No. DE-NA0001974 and DOE-BES under Award No. DE-FG02-99ER45775, with partial instrumentation funding by NSF. APS is a U.S. DOE Office of Science User Facility operated for the DOE Office of Science by ANL under Contract No. DE-AC02-06CH11357." Sample preparation at LANL was performed under the auspices of the U.S. DOE, OBES, Division of Materials Sciences and Engineering.

References

[1] A. J. Arko, J. J Joyce, L. Havela, *The Chemistry of the Actinide and Transactinide Elements*, eds L. R Morss, N. M Edelstein, and J Fuger (Springer, The Netherlands), **Vol 4**, pp 2307–2379 (2006).

[2] V. Sechovsky V and L. Havela, *Handbook of Magnetic Materials*, ed K. H. J. Buschow (North-Holland Amsterdam) **Vol. 11**, chapter 1 (1998).

[3] H. H. Hill, *The 'early' actinides; The Periodic System's f electron transition metal series*, in Plutonium and Other Actinides, edited by W.N. Miner, (AIME, New York) (1970).

[4] J.M. Leger, I. Vedel, A.M. Redon, J. Rossat-Mignod, O. Vogt, Solid State Communications, **66**, No. 11, pp. 1173-l 176, (1988).

[5] A. V. Kolomiets, J.-C. Griveau, S. Heathman, A. B. Shick, F. Wastin, P. Faure, V. Klosek, C. Genestier, N. Baclet and L. Havela, EPL, 82, 57007 (2008).

[6] J. D. Thompson, J. L. Sarrao, N. J. Curro, E. D. Bauer, L. A. Morales, F. Wastin, J. Rebizant, J. C. Griveau, P. Boulet, E. Colineau, G. H. Lander, *Superconductivity in actinide materials*, in: R. Alvarez, N.D. Bryan, I. May (Eds.), *Recent Advances in Actinide Science*, Royal Society of Chemistry, Cambridge, (2006).

[7] Z. Fisk, G. R. Stewart, J. O. Willis, H. R. Ott, and F. Hulliger, Phys. Rev. B **30**, 6360 (1984).

[8] J. D. Thompson, A. C. Lawson, M. W. McElfresh, A. P. Sattelberger, and Z. Fisk, J. Magn. Magn. Mater. **76-77**, 437 (1988).

[9] J. D. Thompson, Z. Fisk, M. W. McElfresh, H. R. Ott, and M. B. Maple, Phys. Rev. B **39**, 2578 (1989).

[10] C. R. Rotundu, B. Andraka, G. R. Stewart, Y. Takano and Z. Fisk, J. Appl. Phys **97**, 10A912 (2005).

[11] E.Yamamoto, Y. Hirose, K. Enoki, K. Mitamura, K. Sugiyama, T. Takeuchi, M. Hagiwara, K. Kindo, Y. Haga, R. Settai, and Y. Ōnuki, J. Phys. Soc. Jpn. **81**, SB023 (2012).

[12] A. L. Cornelius, A. J. Arko, J. L. Sarrao, and N. Harrison, Phys. Rev. B **59**, 13542–13545 (1999).

[13] B. Andraka, G. R. Stewart, and Z. Fisk, Phys. Rev. B **44**, 10346 (1991).

[14] Y. Hirose, Y. Miura, H. Tsutsumi, S. Yoshiuchi, M. Ohya, K. Sugiyama, T. Takeuchi, H. Yamagami, E. Yamamoto, Y. Haga, R. Settai and Y. Ōnuki, Phys. Status Solidi B, **250**, Issue 3, 642–645 (2013).

[15] H. R. Ott and Z. Fisk, in Handbook on the Physics and Chemistry of the Actinides, edited by A. J. Freeman and G. H. Lander (North-Holland, Amsterdam, 1987), **Vol. 5**, Chap. 2, p. 85.

[16] E.Yamamoto, Y. Hirose, K. Enoki, K. Mitamura, K. Sugiyama, T. Takeuchi, M. Hagiwara, K. Kindo, Y. Haga, R. Settai, and Y. Ōnuki, J. Phys. Soc. Jpn. **81**, SB023 (2012).

[17] J-P. Rueff and A. Shukla, Rev. Mod. Phys. **82**, 847-896 (2010).

[18] B.T. Thole, G. van der Laan, J.C. Fuggle, G.A. Sawatzky, R.C. Karnatak, and J.-M. Esteva, Phys. Rev. B **32**, 5107 (1985).

[19] M. O. Krause and J. H. Oliver, J. Phys. Chem. Ref. Data, **8**, 328 (1979).

[20] O. Keski-Rahkonen, M. O. Krause, Atom Data Nucl. Data Tables, **14,** 139–146 (1974).

[21] C.H. Booth, Yu Jiang, D.L. Wang, J.N. Mitchell, P.H. Tobash, E.D. Bauer, M.A. Wall, P.G. Allen, D. Sokaras, D. Nordlund, T. C. Weng, M.A. Torrez, and J.L. Sarrao, PNAS, **109**, no. 26, 10205– 10209 (2012).

[22] C.H. Booth, S.A. Medling, Yu Jiang, E.D. Bauer, P.H. Tobash, J.N. Mitchell, ,D.K. Veirs, M.A. Wall, P.G. Allen, J.J. Kas, D. Sokaras, D. Nordlund, T.-C. Weng, Journal of electron spectroscopy and related Phenomena, **194**, 57-65 (2014).

[23] Ashcroft, N. W. and Mermin, N. D., *Solid State Physics*, (Philadelphia: Saunders College), pp 47 (1976).

[24] P. C. Canfield, Z. Fisk, Philos. Mag. B, **65**, 1117–1123 (1992).

[25] Y. M. Xiao, P. Chow, G. Boman, L. G. Bai, E. Rod, A. Bommannavar, C. Kenney-Benson, S. Sinogeikin, and G. Y. Shen, Review of scientific instruments **86**, 072206 (2015).

[26] D. Haskel (May 1999) *FLUO: Correcting XANES for self-absorption in fluorescence data*. http://www.aps.anl.gov/xfd/people/haskel/fluo.html

[27] A. Jayaraman, Rev. Mod. Phys., **55**, No. 1, January (1983).

[28] A. P. Hammersley, S. O. Svensson, M. Hanfland, A. N. Fitch, and D. Hausermann, High Pressure Research, **14**, 235–248 (1996).

[29] P. Dera, B. Lavina, L. A. Borkowski, V. B. Prakapenka, S. R. Sutton, M. L. Rivers, R. T. Downs, N. Z. Boctor, and C. T. Prewitt, Geophys. Res. Lett. **35**, L10301 (2008).

[30] P. Dera, B. Lavina, L. A. Borkowski, V. B. Prakapenka, S. R. Sutton, M. L. Rivers, R. T. Downs, N. Z. Boctor, and C. T. Prewitt, Geophys. Res. Lett. **35**, L10301 (2008).

[31] Y. Meng, G. Shen and H. K. Mao, J. Phys.: Condens. Matter **18**, S1097–S1103 (2006).

[32] S. Bertram, G. Kaindl, G. Schmiester and O. Vogt. High Pressure Research, **2**, pp 361-365 (1990)

[33] A. Krimmel, A. Loidl, K. Knorr, B. Buschinger, C. Geibel, C. Wassilew and M. Hanfland, J. Phys.: Condens. Matter 12, 8801–8808 (2000).

[34] J.-P. Rueff, S. Raymond, A. Yaresko, D. Braithwaite, Ph. Leininger, G. Vankó, A. Huxley, J. Rebizant, and N. Sato, Phys. Rev. B, **76,** 085113 (2007).

[35] G. Kalkowski, G. Kaindl, W.D. Brewer, and W. Krone, Phys. Rev. B, **35**, 2667 (1987).

[36] J. F. Herbst and J.W. Wilkins, Phys. Rev. B, **38**, 1027 (1988)

[37] P. Söderlind, A. Landa, J. G. Tobin, P. G. Allen, S. Medling, C. Booth, J. Cooley, E. D. Bauer, D. Sokaras, T.-C. Weng, D. Nordlund (preprint).

[35] F. Birch, Phys. Rev., **71**, 809 (1947).

[36] P. Vinet, J. Ferrante, J.R. Smith, and J.H. Rose, J. Phys. **C 19**, L467 (1986).

[37] P. Vinet, J. Ferrante, J.H. Rose, and J.R. Smith, J. Geophys. Res. **92**, 9319 (1987).

[38] U. Benedict, S. Dabos, L. Gerward, J. Staun Olsen, J. Beuers, J. C. Spirlet, C. Dofour, J. of Magn. and Magn. Mat. Materials, **63 & 64,** 403 (1987).

[39] S S. Heathman, M. Idiri, J. Rebizant, P. Boulet, P. S. Normile, L. Havela and V. Sechovsky´, T. Le Bihan, Phys. Rev. B **67**, 180101(R) (2003).

[40] N. Tateiwa, S. Ikeda, Y. Haga, T. D. Matsuda, M. Nakashima, D. Aoki, R. Settai, Y. Onuki, J. of Physics: Conference Series, **150**, 042206 (2009).

[41] A. Dewaele, J. Bouchet, F. Occelli, M. Hanfland, and G. Garbarino, Phys. Rev. B **88**, 134202 (2013).

[42] G. Bellussl, U. Benedict and W. B. Holzapfel, J. Less-Common Metals **78**, 147 (1981).

[43] W. J. Evans, M. J. Lipp, H. Cynn, and C. S. Yoo, M. Somayazulu and D. Häusermann, G. Shen and V. Prakapenka, Phys. Rev. B, **72**, 094113 (2005).

[44] *Tables of Physical & Chemical Constants* (16th edition 1995). 2.2.2 Elasticities and strengths. Kaye & Laby Online. Version 1.0 (2005) www.kayelaby.npl.co.uk

Figure Captions

Fig. 1. $BaHg_{11}$-type cubic structure of UCd_{11} with a lattice constant of 9.29 Å**.** The uranium atom occupies the 3c position having tetragonal symmetry and has 12 nearest-neighbors and 8 next-nearest neighbor Cd atoms.

Fig. 2. PFY-XAS spectra at uranium L_3 edge for UCd_{11} compound at different pressures.

Fig. 3. Pressure dependence of shift (E_{LIII}) of white line position in PFY-XAS spectra with respect to ambient white line position taken as reference ($E_{LIII} = 0$).

Fig. 4. Pressure dependence of the full width at half maxima (FWHM) of white line in PFY-XAS spectra.

Fig. 5. Pressure dependence of normalized unit cell volume of UCd_{11} compound. The open circles are experimental data and solid lines are fit to Vinet (green) and 3rd order Birch-Murnaghan (red) equation of state (EOS). Both fits overlap each other. The error bars on V/V_0 are much smaller than the dimension represented by the symbol.

Fig. 6. Images of SXD peaks at (a) 1.5 GPa and (b) 12.7 GPa. The circular image shows the complete reflections collected while rotating the sample about an axis perpendicular to the beam. The rectangular images on the right show zoomed in portions of some indexed reflections. Black squares mark in zoomed portion are indexed reflections. All the reflections could be indexed but only certain h k l range is chosen here for clarity.

Fig. 7. Comparison of the profile of a SXD peak at two different pressure 1.5 GPa and 12.7 GPa.

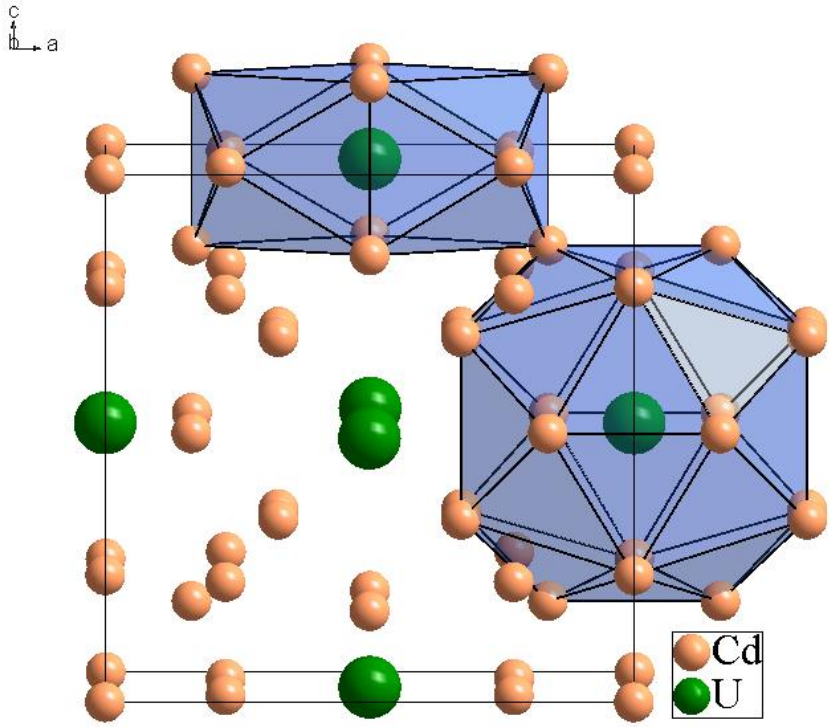

Figure 1

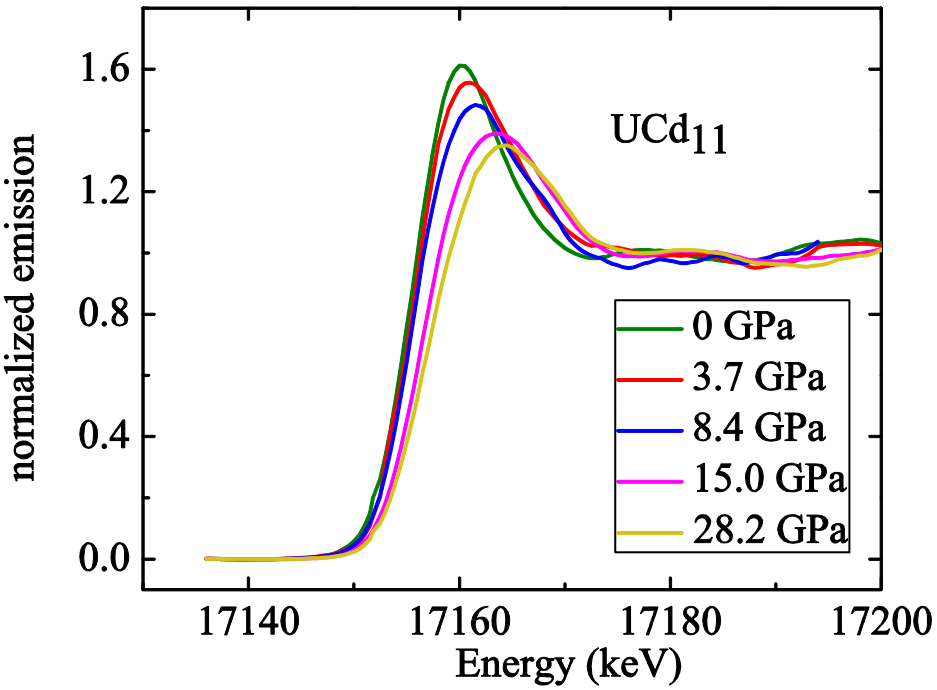
normalized emission
1.6
1.2
0.8
0.4
0.0
UCd11
0 GPa
3.7 GPa
8.4 GPa
15.0 GPa
28.2 GPa
17140
17160
17180
17200
Energy (keV)

Figure 2

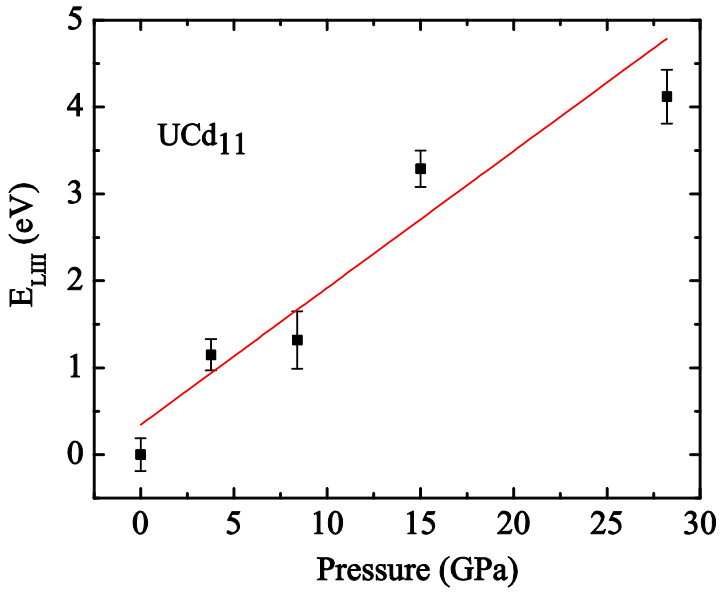

Figure 3

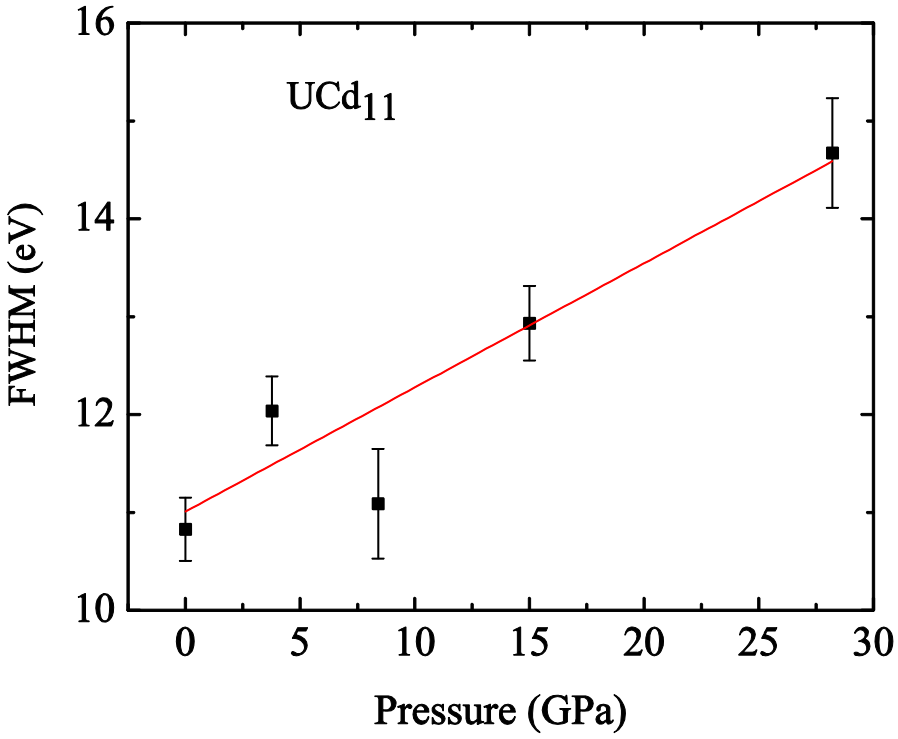

Figure 4

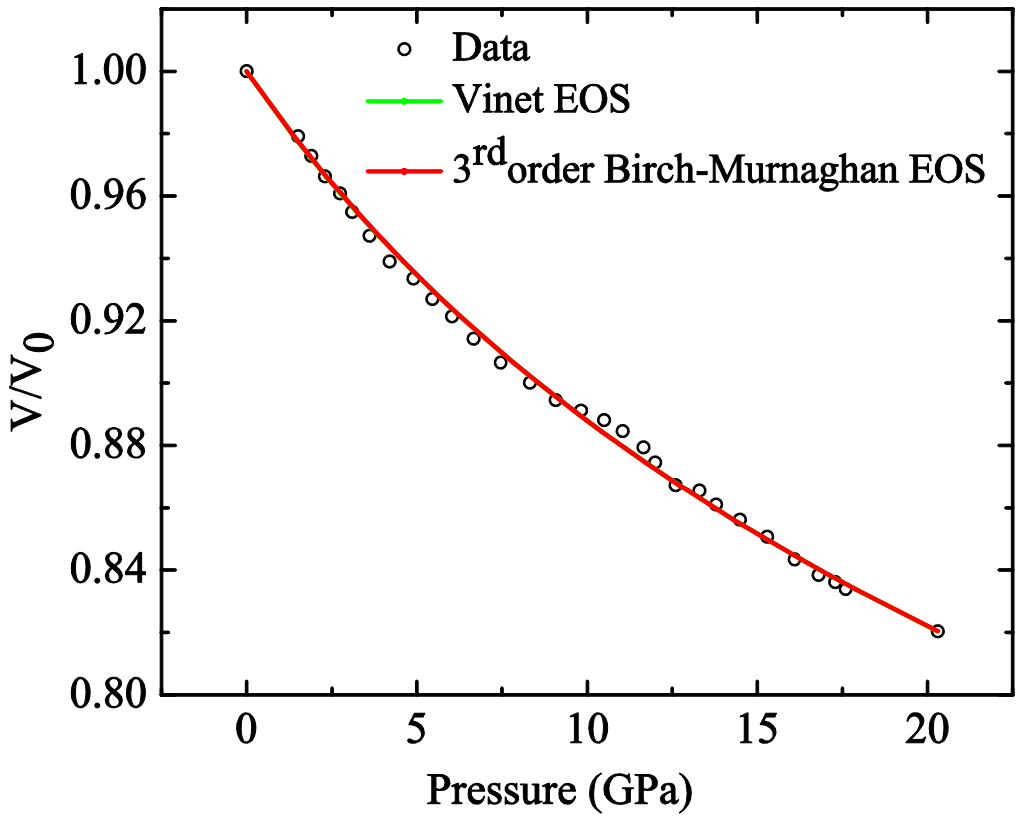
Data
Vinet EOS
3rd order Birch-Murnaghan EOS
V/V0
1.00
0.96
0.92
0.88
0.84
0.80
0
5
10
15
20
Pressure (GPa)

Figure 5

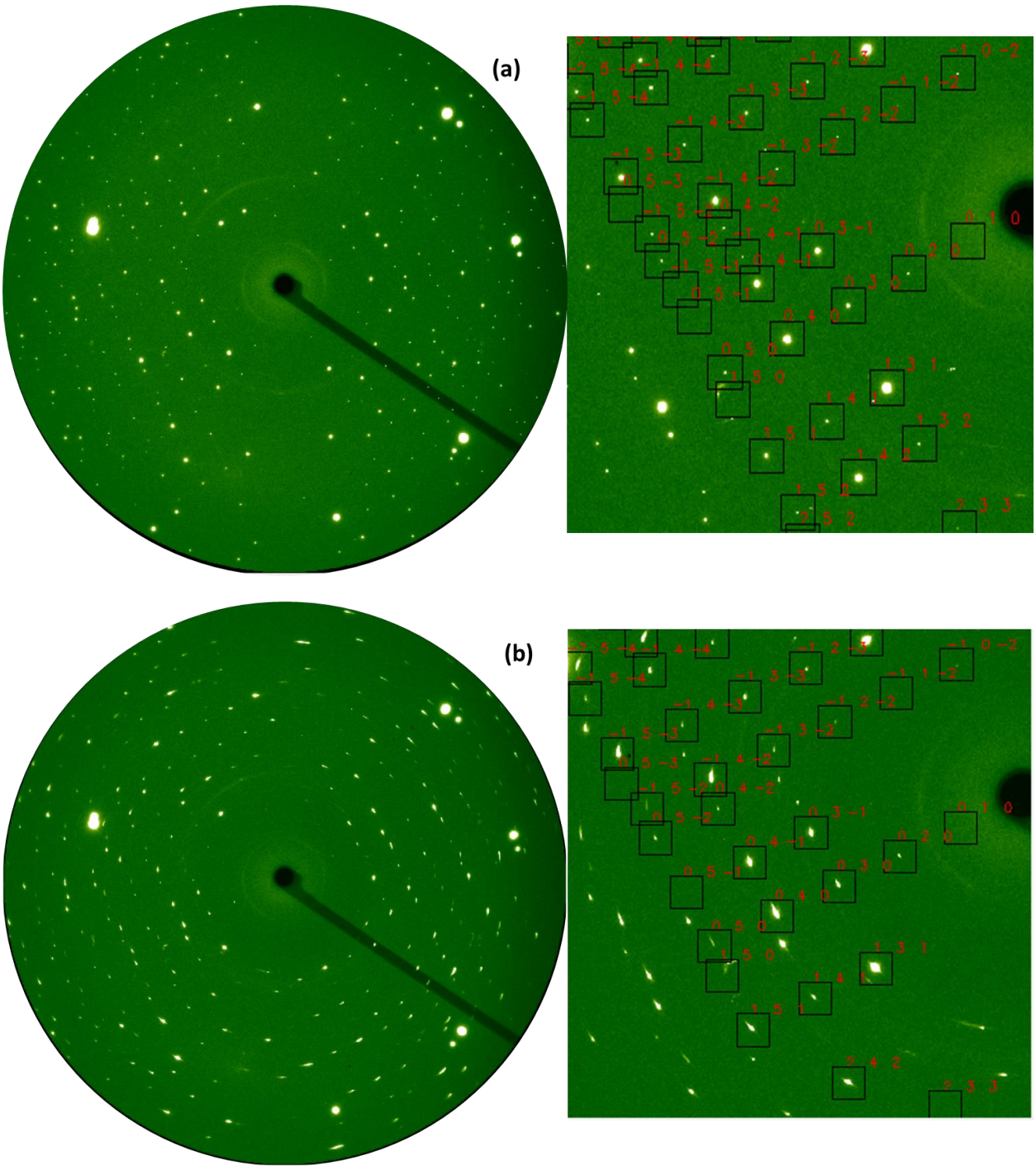

Figure 6

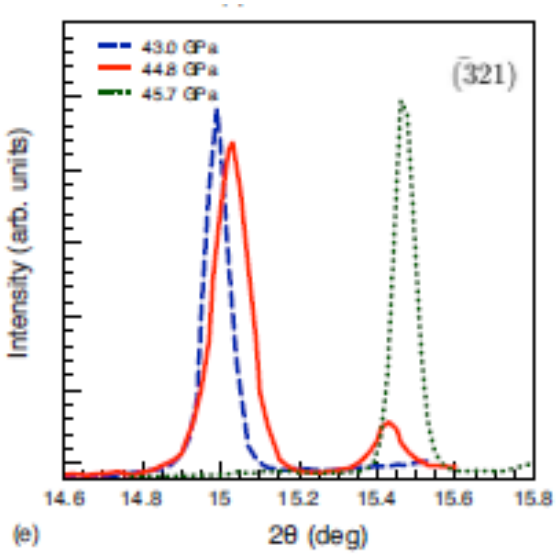

Figure 7

This is not for my sample; I will try to add a similar figure for UCd_{11}.